Self-assembly, stability quantification, controlled molecular switching, and sensing properties of an anthracene-containing dynamic [2]rotaxane†

Wing-Yan Wong,[a] Ken Cham-Fai Leung*[a] and J. Fraser Stoddart*[b]

Received 22nd December 2009, Accepted 18th February 2010
First published as an Advance Article on the web 19th March 2010
DOI: 10.1039/b926568f

The preparation of a novel anthracene-containing dynamic [2]rotaxane by a templating self-assembly process between a diamine and a dialdehyde to form a [24]crown-8 macrocyclic diimine, in the presence of a dumbbell containing a secondary dialkylammonium ion center as the template, which has been exploited for its sensing properties. By appealing to the ability of the anthracene ring system—one of the two stoppers associated with the dumbbell—to act as a fluorescent probe, the fluorescence and fluorescence-quenching nature of the dynamic rotaxane in an equilibrium mixture has been investigated and quantified in the presence of external stimuli such as water, acids, salts, and an amine. The stability, as expressed by the hydrolysis of the dynamic rotaxane has been monitored by following: (i) the anthracene fluorescence and (ii) the movements of the signals in the ^{1}H NMR spectra. The rate of hydrolysis ($t_{1/2}$ = 6.9 min) of the dynamic rotaxane in the presence of a small amount (1 equiv.) of acid was found to be very much faster than when the hydrolysis was carried out with a large amount (>100 equiv.) of water, when $t_{1/2}$ > 140 min. Furthermore, it has been established that the anthracene fluorescence of the dynamic rotaxane rises with an increasing amount of acid. Two acid sensors have been identified with different operating modes—namely, logarithmic and linear. The combination of different inputs involving water, acids, salts and an amine leads to different fluorescence outputs from the dynamic rotaxane, hence, producing a prototype for expressing molecular logic.

Introduction

Recently, dynamic covalent chemistry (DCC) has attracted[1] increasing attention on account of its usefulness when it comes to producing compounds, such as molecular Borromean rings,[2] some selected dendrimers,[3] and other exotic products,[4] in a highly efficient manner using one-pot, multicomponent, templated, self-assembly processes.[5] The nearly quantitative formation of (super)structures with mechanically intertwined and interlocked entities indicates that the template effect[5b] is highly efficient, yielding thermodynamically stable supramolecular intermediates. The main advantage of the thermodynamic process over the kinetic one is that the former operates under (reversible) equilibrium control, such that the formation of undesired or competitive intermediates will eventually be transformed into the most energetically favoured products by error checking and proof reading.[1h]

DCC relies upon the use of covalent bonds that form and break in a completely reversible manner during a particular reaction step in a synthesis. Common dynamic equilibrating (reversible) reactions exploited in such syntheses include olefin metathesis,[6] and disulfide[7] and imine[8] bond formation. Generally, imines are relatively unstable and undergo rapid hydrolysis in the presence of water.[9] However, attention has been drawn[10] recently to the fact that imine-containing macrocycles possess remarkable stabilities in the presence of water. Other systems,[11] involving dative coordination bonds between imines and transition metal ions,[12] can also experience increased imine bond stability in aqueous solutions. The pH control[13] over the structure and properties of some of these compounds, as a result of molecular switching in aqueous solutions, may offer practical applications in, for example, microfluidic devices.[14]

The interaction between light and designed supramolecular systems exploits the energy and information content of photons.[15] In one particular mode, a photoreaction occurring in a supramolecular system causes some changes in the properties of the system, which are reflected in a monitorable signal. Moreover, interaction between supramolecular self-assemblies of components affects photoresponses, a property which can be revealed by some form of excited state manifestation—often luminescence. In supramolecular systems, the photo-physicochemical properties of each component can be modified profoundly upon complexation. Such changes can be useful in obtaining information on the superstructure of a complex, and also in assisting in the design of sensors for practical applications.[16]

Based on our previous investigations on the high-yielding synthesis of [2]rotaxanes employing thermodynamic templated syntheses,[8] we report here the synthesis and characterisation of an anthracene-containing dynamic [2]rotaxane. Our interest in the development of photochemical molecular and supramolecular devices, together with studies on photoenergy- and electron-transfer processes in supramolecular systems,[17] has led us to

[a]*Center of Novel Functional Molecules, Department of Chemistry, The Chinese University of Hong Kong, Shatin, NT, Hong Kong SAR, P. R. China. E-mail: cfleung@cuhk.edu.hk; Fax: (+852) 2603-5057*
[b]*Department of Chemistry, Northwestern University, 2145 Sheridan Road, Evanston, Illinois 60208, USA. E-mail: stoddart@northwestern.edu; Fax: (+1) 847-491-1009*

† Electronic supplementary information (ESI) available: Experimental procedures, analytical and spectral characterisation data, and expanded discussions of peripheral findings and control experiments. See DOI: 10.1039/b926568f

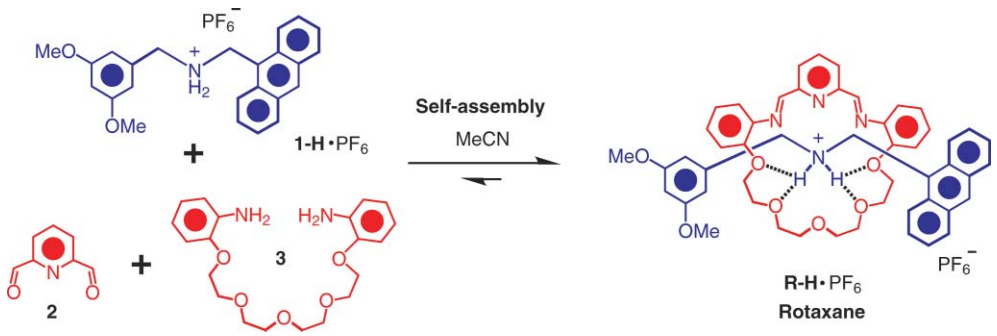

Scheme 1 Thermodynamically driven formation of the rotaxane **R-H**·PF_6.

explore: (i) the stability, (ii) exchange dynamics and (iii) switching in this dynamic [2]rotaxane in the presence of various stimuli, *e.g.*, water, salts, acids, and amines.

Results and discussion

Scheme 1 summarises the template-directed synthesis[18] of the [2]rotaxane **R-H**·PF_6, incorporating a photosensitising anthracene unit as one of the two stoppers on its dumbbell component. It involves the self-assembly of 2,6-diformylpyridine (**2**) and the diamine **3** in MeCN in the presence of the secondary dialkylammonium salt **1-H**·PF_6. The resulting [24]crown-8-like macrocycle is amplified as a result of the highly selective [1 + 1] condensation between **2** and **3**, and becomes interlocked mechanically around the template ion **1-H**$^+$. The 3,5-dimethoxyphenyl group serves as the other bulky stopper and the rotaxane **R-H**·PF_6, constituted of a macrocyclic diimine surrounding the dumbbell-shaped component, is the outcome ultimately of the equilibrium-controlled reaction. The thermodynamic stability of the rotaxane arises as a result of complementary recognition associated with [N^+–H···X] hydrogen bonds and [N^+C–H···O] interactions (X = O or N), in addition to electrostatic and C–H···π interactions[8c] between the [24]crown-8-like macrocycle and the dumbbell component.

An equilibrated (5 min) equimolar (60 mM) mixture of **1-H**·PF_6, **2** and **3** in MeCN yielded a mass spectrum (Fig. S1, ESI†) in which a singly charged molecular ion base peak (m/z) of 833 reveals the formation of the **R-H**$^+$ ion, having lost its PF_6^- counterion. No significant higher mass signals were observed, indicating that no other higher-order macrocyclic homo-oligomers or related acyclic oligomers were formed.

The formation of **R-H**·PF_6 is also supported by ^{1}H NMR spectroscopy carried out on an equilibrating equimolar mixture of the three starting materials in CD_3CN. The spectrum (Fig. 1) of the rotaxane shows the emergence[8c] of new sharp resonances which are very different from those of the starting materials, namely **1-H**·PF_6, **2** and **3**. The nature of these new resonances suggests that **R-H**$^+$ is the thermodynamically most stable product of the reaction mixture. In particular, the characteristic signal for the benzylic methylene group protons (H_d/H_e) adjacent to the NH_2^+ center are shifted from $\delta = 4.4$ and 5.2 ppm in **1-H**$^+$ to $\delta = 5.1$ and 5.8 ppm in **R-H**$^+$. Moreover, the formyl proton (C*H*O) resonance (δ = 10.1 ppm) in **2** disappears in the spectrum of the product, while the corresponding imine (H_i) resonance ($\delta = 7.9$ ppm) becomes a prominent and predominant signal. The sharpness of the peaks for the rotaxane in the ^{1}H NMR spectrum indicates that it is stable kinetically on the ^{1}H NMR time scale. We conclude from this experiment that the formation of **R-H**·PF_6 proceeds in >90% yield.

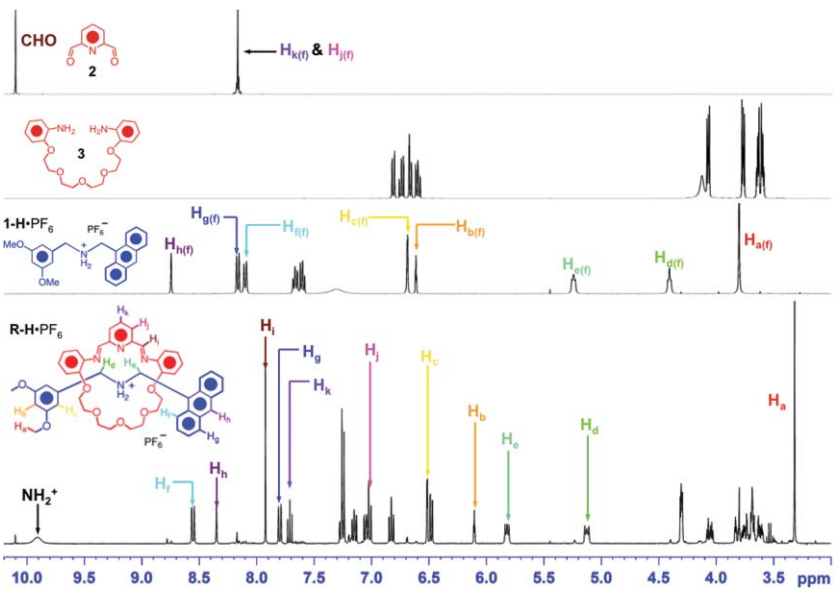

Fig. 1 ^{1}H NMR spectra (400 MHz, CD_3CN, 295 K) of **R-H**·PF_6 and its free components: dumbbell **1-H**·PF_6, dialdehyde **2** and diamine **3** (f = free).

In order to elucidate the absorption and emission characteristics of the multicomponent rotaxane, reference has to be made to the starting materials and a suitable model compound, *e.g.*, the open-chain analogue **4** of the macrocycle. The UV/Vis absorption spectrum (Fig. 2) of **R-H**·PF_6 is not all that dissimilar from the sum of the separate components. In particular, the absorption spectra of **R-H**·PF_6 and **1-H**·PF_6 both show the characteristic band at 300–400 nm which originates from the anthracene moiety.[17] Upon excitation at 290 nm, where most of the light is absorbed by the components, anthracene fluorescence ($\lambda_{max} = 418$ nm) is observed (Fig. 3) in the case of **1-H**·PF_6, whereas the aminophenolic residues fluoresce at $\lambda_{max} = 334$ nm for **3**, **4** and **R-H**·PF_6. By contrast, the anthracene fluorescence of the rotaxane is completely quenched. It is well known[18] that when anthracene is in close proximity to an amino group, quenching occurs by electron transfer from that group. Here, the anthracene fluorescence quenching in **R-H**·PF_6 is presumably being caused by electron transfer from the imine and pyridine moieties in the macrocycle. Since the solutions are extremely dilute, intermolecular quenching can be ruled out. The anthracene fluorescence of the dumbbell **1-H**·PF_6 is not quenched by the physical mixing of it with **2**, **3** or **4**, separately (Fig. S4, ESI†).

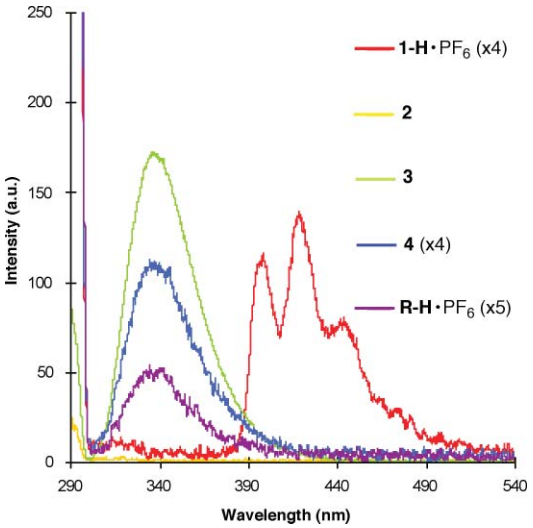

Fig. 3 Fluorescence emission spectra (excitation wavelength = 290 nm) of components (conc. = 0.02 mM in MeCN).

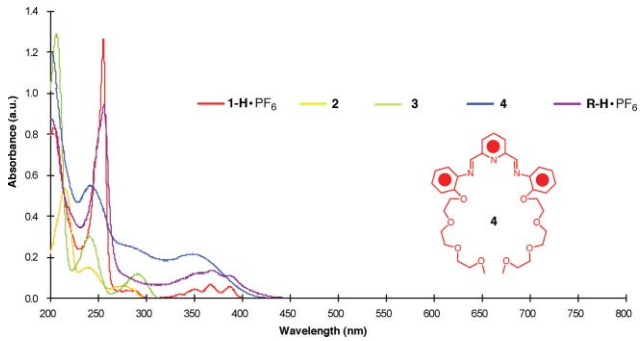

Fig. 2 UV/visible absorption spectra (conc. = 0.02 mM in MeCN) of components.

By monitoring the anthracene fluorescence intensity in the equilibrium mixture of the reactants and products, we can get a handle on the relative concentrations of the rotaxane and its separate components based on the fact that the dumbbell is fluorescent while the rotaxane is fluorescence quenched. A dissociation mechanism for the rotaxane in the presence of water is shown in Scheme 2. The kinetically labile imine bonds in the rotaxane can be broken and reformed in the presence of water molecules, affording the intermediates **I** and **II** which may also possess some residual stability as a result of the noncovalent bonding interactions, until the separate components are further fragmented and dissolved in the solvent system.

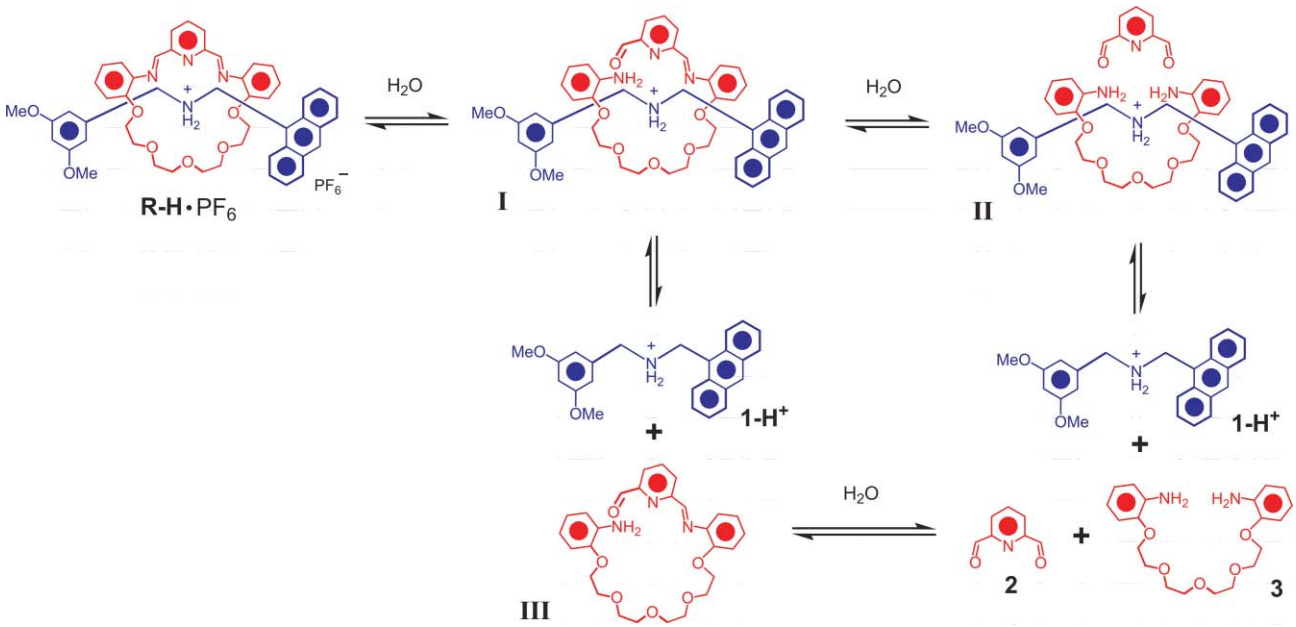

Scheme 2 Stability through dissociation of **R-H**·PF_6 and its intermediates **I**, **II** and **III**.

The fluorescence emissions of the dumbbell and the rotaxane were monitored after treatment with an excess (~200 equiv.) of water or acid (1.0 M HCl). Anthracene fluorescence bands are observed (Fig. 4) for the dumbbell when it is mixed separately with an excess of water or acid. No fluorescence quenching occurs. The slight decrease in fluorescence intensity of the dumbbell on addition of an excess of water compared to the dumbbell free of water may be attributed to a dilution effect. There is a significant increase, however, in the fluorescence intensity on the addition of excess acid compared to the dumbbell free of acid. This observation may be attributed to the partial protonation of the methoxy groups of the dumbbell such that intramolecular electron transfer from these groups to the anthracene is deactivated. On the other hand, when the rotaxane was treated with an excess of water, the anthracene fluorescence is completely quenched. By contrast, anthracene fluorescence is observed when the rotaxane is treated with an excess of acid.

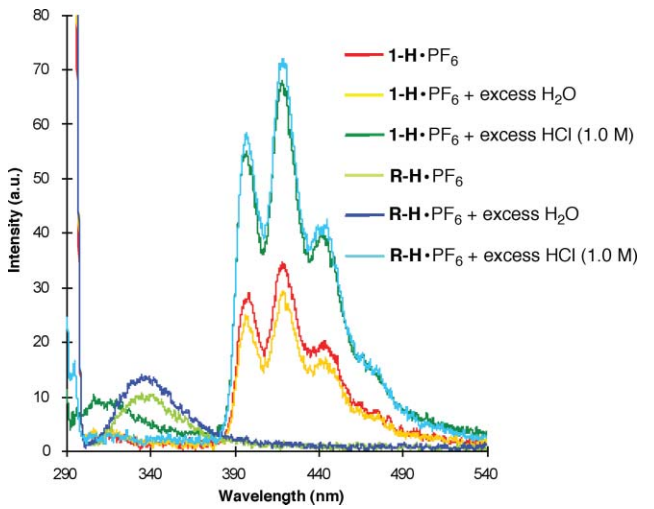

Fig. 4 Fluorescence emission spectra (excitation wavelength = 290 nm) of components (conc. = 0.02 mM in MeCN).

Finally, addition of base (NaOH, Et_3N, *etc.*) to the rotaxane leads to the deprotonation of the dumbbell, whereupon its templating role is lost, leading to its dissociation into its components. The deprotonated dumbbell is fluorescence quenched because the covalently linked secondary amine deactivates the lower lying anthracene fluorescence. Thus, its fluorescence cannot be observed in the presence of water or base, only in the presence of acid.

Dissociation of rotaxane in the presence of water

Since fluorescence spectroscopy reveals (Fig. 4) that the anthracene fluorescence of the rotaxane is quenched in the presence of excess water, a dissociation mechanism (Scheme 3) can be drawn in which the equilibrium is displaced towards the rotaxane and intermediate **I**, in keeping with their fluorescence quenching properties. The intermediate **III** is presumably likely to dissociate to the dialdehyde **2** and the diamine **3** in the presence of water because of the loss of the template effect.

The equilibrated mixture (CD_3CN, 0.02 mM) in the presence of excess of D_2O was probed using ^1H NMR spectroscopy. The spectrum (Fig. 5) reveals sets of signals which correspond to all of the components. Integration of these signals, however, demonstrates that the rotaxane is still the dominant species in the mixture. The additional signal at $\delta = 10.05$ ppm can be attributed to the monoaldehyde (C*H*O) proton in the intermediate **I** (Scheme 3). The rotaxane shows remarkable stability in water.[8c] The hydrolysis of the rotaxane is a reversible process. Removal of the water from the reaction mixture with drying agents, such as anhydrous Na_2SO_4, does not jeopardize the break-down products, which duly recombine to produce the rotaxane once again when water is removed.

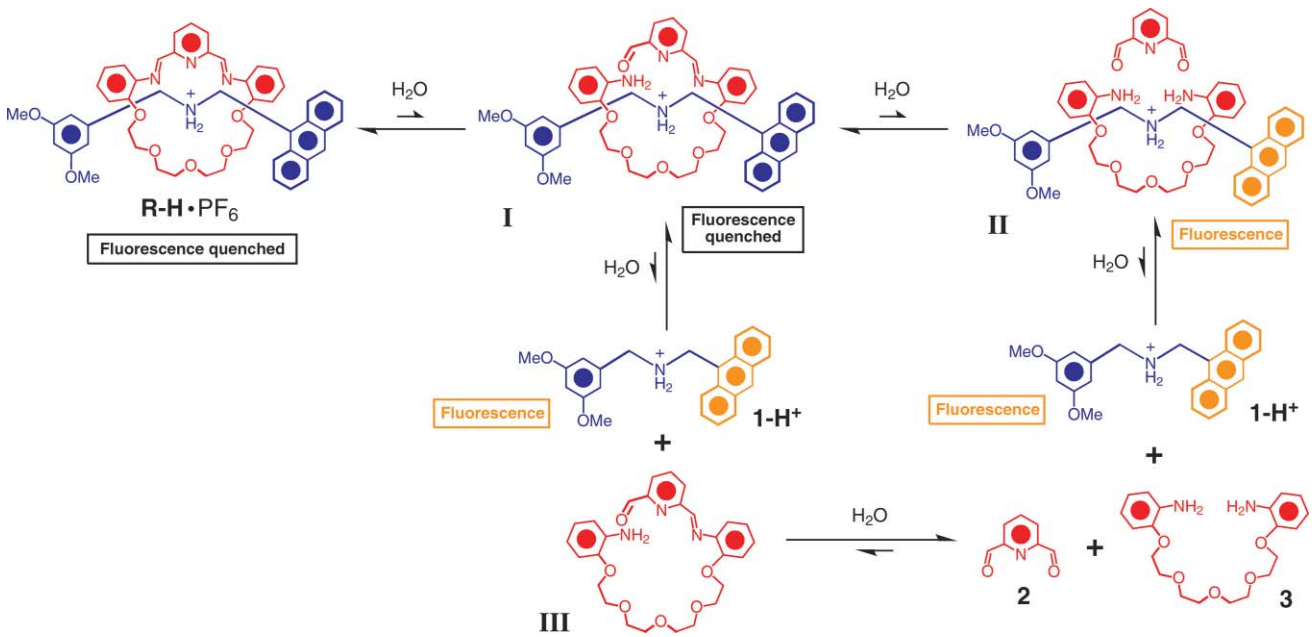

Scheme 3 Dissociation mechanism and fluorescence quenching of **R-H**·PF_6 in the presence of water. The equilibrium favours the formation of **R-H**·PF_6 from which the anthracene fluorescence is quenched.

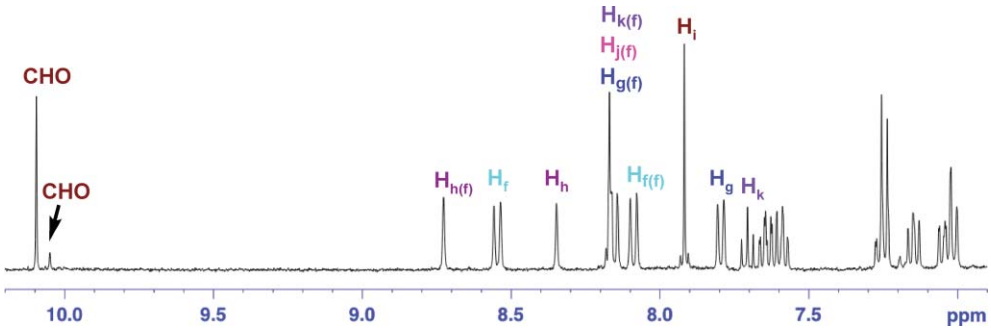

Fig. 5 Partial ^{1}H NMR spectrum (400 MHz, CD_3CN, 295 K) of **R-H**·PF_6 in the presence of excess of D_2O (f = free).

Dissociation of rotaxane in the presence of acid/water

Fluorescence spectroscopy reveals (Fig. 4) that the anthracene fluorescence was observed once again when the rotaxane was treated with an excess of acid (1.0 M HCl). We have found out—in an experiment designed to compare counterion and acidity effects—that the use of 0.1 M HPF_6 (a weaker acid) for rotaxane dissociation also results in anthracene fluorescence. It is believed that the addition of NH_4PF_6 (a weak acid) would also trigger dissociation[8b] of the rotaxane. A dissociation mechanism (Scheme 4) can be proposed in which the equilibrium favours the formation of the separate components, namely, **1-H**$^+$, **2** and **3**, and so accounts for the observation of anthracene fluorescence. The equilibrated mixture (in CD_3CN) in the presence of 1.0 equiv. HCl/H_2O (0.5 M) was examined by ^{1}H NMR spectroscopy. The spectrum (Fig. 6a) reveals sets of signals for all of the equilibrating components. From ^{1}H NMR integrations, the rotaxane turns out to be the least dominant species in the mixture. The weak signal resonating at $\delta = 10.12$ ppm can be assigned to the monoaldehyde (C*H*O) proton in the intermediate **III** (Scheme 4). By contrast, the ^{1}H NMR spectrum (Fig. 6b) of the equilibrated mixture in the presence of excess of HPF_6/H_2O (0.1 M) reveals that the rotaxane is dissociated entirely into its components. Slight shifts in the ^{1}H NMR resonances are observed on account of a counterion effect. In particular, the weak residual monoaldehyde (C*H*O) signal resonates at $\delta = 10.00$ ppm.

The change in the rotaxane concentration resulting from dissociation using either water or aqueous acid was monitored (Fig. 7) by ^{1}H NMR spectroscopy. The dissociation of the rotaxane was confirmed by observing the gradual decrease in the intensity of the imine signal ($\delta = 7.92$ ppm) intensity with the consequent increase in the intensity of the aldehyde resonance ($\delta = 10.10$ ppm) and the shifts of the N^+C–H signals from $\delta = 5.1$ (H_d) and 5.8 ppm (H_e) to $\delta = 4.4$ ($H_{d(f)}$) and 5.2 ppm ($H_{e(f)}$), respectively.

Fig. 8 shows a plot of rotaxane concentration *versus* time while D_2O or HCl/H_2O were being added. ^{1}H NMR spectroscopic signals are tracked. On addition of water or aqueous acid to the rotaxane in CD_3CN solution, equilibria were reached generally after about 5 h. In particular, it requires the presence of over 200 equiv. of water for the rotaxane to become half dissociated.

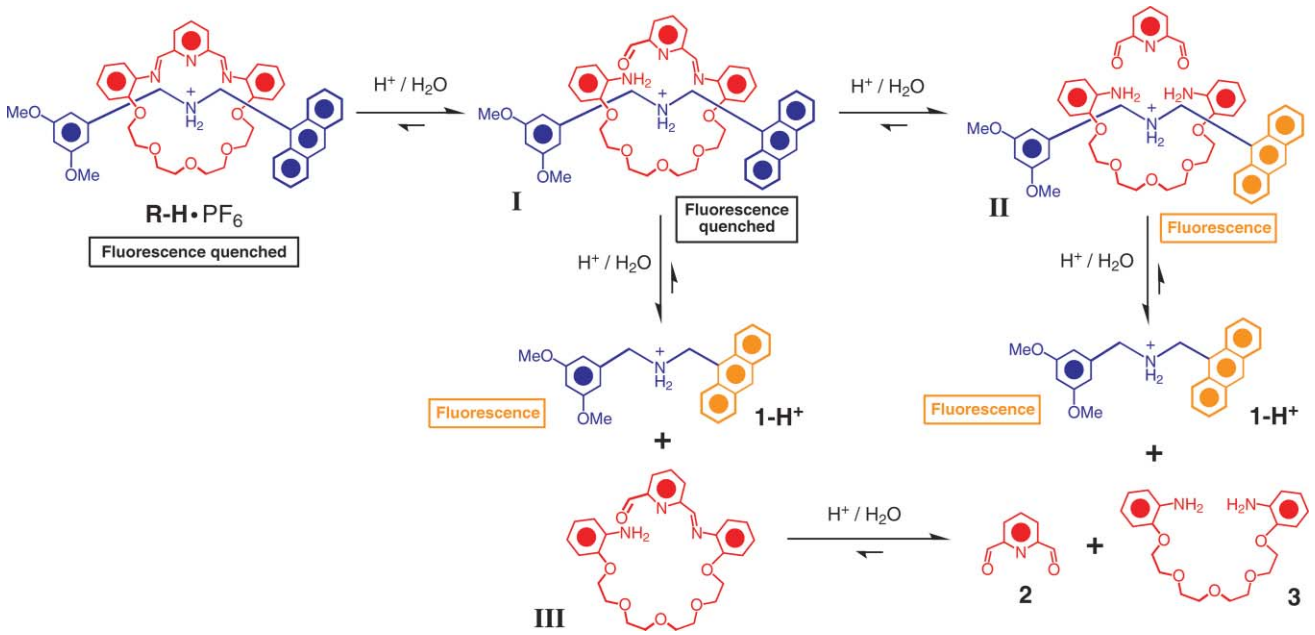

Scheme 4 Dissociation mechanism and fluorescence quenching of **R-H**·PF_6 in the presence of acid/water (1.0 M HCl or 0.1 M HPF_6). The equilibrium favours the dissociation of **R-H**·PF_6 to give the dumbbell **1-H**·PF_6 from which the anthracene fluorescence is restored.

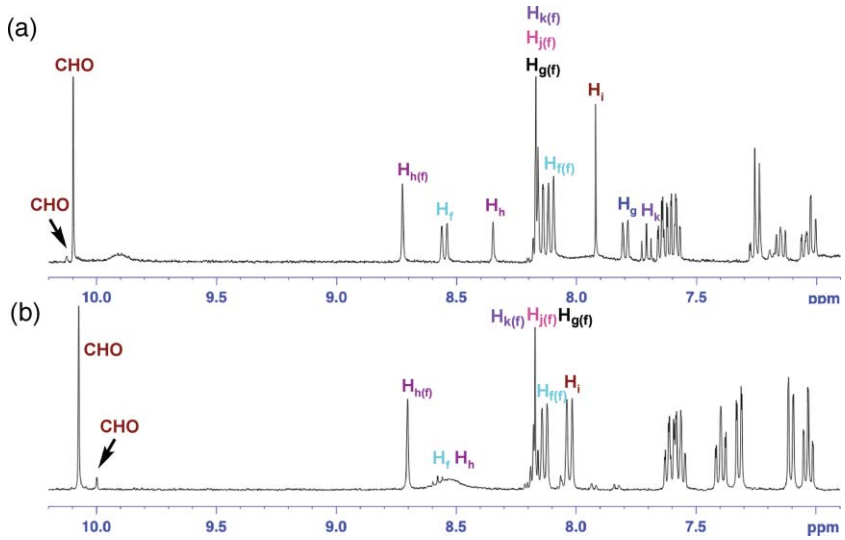

Fig. 6 Partial ^{1}H NMR spectrum (400 MHz, CD_3CN, 295 K) of **R-H**·PF_6 in the presence of (a) 1 equiv. HCl/H_2O (0.5 M) and (b) excess of HPF_6/H_2O (0.1 M) (f = free).

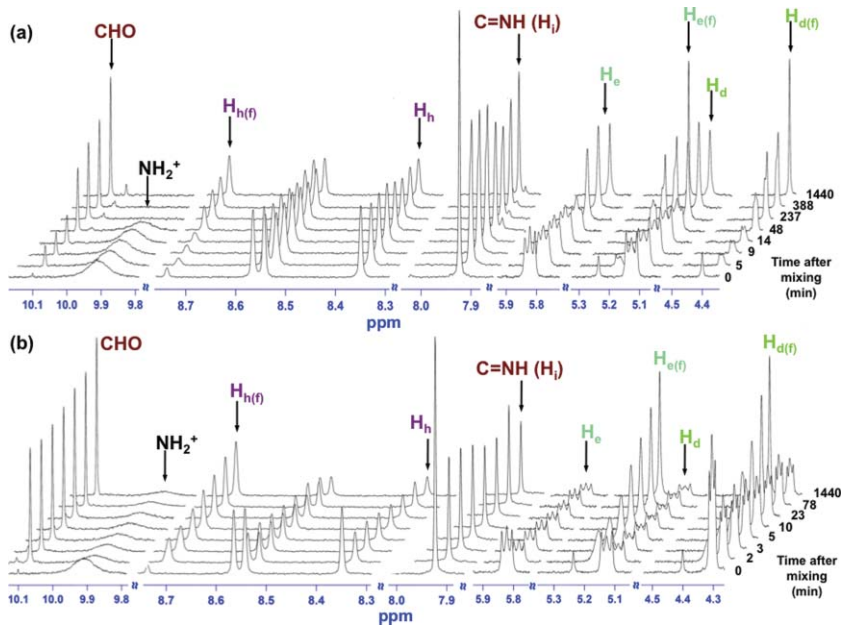

Fig. 7 Stacked partial ^{1}H NMR (400 MHz, CD_3CN, 295 K) plots of **R-H**·PF_6 in the presence of (a) 200 equiv. of D_2O and (b) 1 equiv. of HCl/H_2O (0.5 M) with time.

To be more specific, there are 71, 54 and 24% of the rotaxane remaining at equilibrium in the presence of 100, 200, and 500 equiv. of water. In the beginning, the dissociation rates are rather similar. Upon addition of 1 equiv. of HCl/H_2O (0.5 M) to the rotaxane solution, however, the dissociation rate of the rotaxane was much faster than when employing water alone. The half-lives ($t_{1/2}$) for the dissociation were determined to be, in turn, 149, 132, 78 and 6.9 min for 100, 200, 500 equiv. D_2O and 1 equiv. HCl/H_2O. The reactions within the first hour were shown to follow second-order kinetics from a plot of 1/[**R-H**·PF_6] *versus* time. See Fig. S7 in the ESI.†[8i]

Dissociation of rotaxane in the presence of acid/ether

The stability of the rotaxane has also been examined by dissolving it in anhydrous MeOH, Me_2NCHO (DMF) and Et_2O,[8i] wherein negligible dissociation is observed. The dissociation of the rotaxane was then investigated in excess of anhydrous HCl/Et_2O (0.1 M). To our surprise, the ^{1}H NMR spectrum (Fig. S8, ESI†) of the resulting mixture revealed a complete dissociation of the rotaxane into its separate components. We believe that tiny amounts of water molecules, inevitably present in the mixture, are responsible for the dissociation when the acid is present in excess.

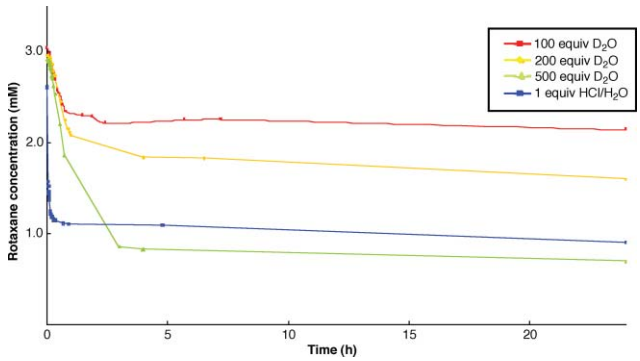

Fig. 8 A plot of the concentration of **R-H**·PF_6 (mM) in CD_3CN *versus* time (h) obtained by ^1H NMR spectroscopy (400 MHz, CD_3CN, 295 K).

Effect of Salt

It occurred to us that dissociation of the rotaxane by competitive binding with a salt, *e.g.*, KPF_6, might offer the possibility of broadening the range of stimuli.[19] The competitive binding would become feasible if the [24]crown-8-like macrocycle were to complex preferentially with K^+ ions, leading to the displacement of the anthracene-containing dumbbell **1-H**·PF_6. The rotaxane and the dumbbell compound were treated successively with excess of KPF_6, H_2O and HCl (1.0 M). The fluorescence spectra show (Fig. S14, ESI†) that when KPF_6 or KPF_6/H_2O were added to the rotaxane **R-H**·PF_6, no anthracene emission was observed. By contrast, the anthracene emission was observed in the presence of HCl (1.0 M) and KPF_6. It follows that KPF_6 has no effect on the rotaxane—that is, the rotaxane does not dissociate to give the free dumbbell, although it does in the presence of acid.

Dissociation of rotaxane by competitive exchange using toluidine

In order to explore the reversible nature of imine exchange, the rotaxane was treated with an amine–toluidine (Tol-NH_2 or *p*-$MeC_6H_4NH_2$). Imine exchange using toluidine during imine formation is expected to inhibit the production of the rotaxane by cleaving the [24]crown-8-like macrocycle. When 2.0 equiv. of toluidine were added to the rotaxane, the ^1H NMR spectrum (Fig. S9, ESI†) revealed new signals at δ = 8.63, 8.21 and 8.01, corresponding to imine (H'_i) and the pyridine aryl (H'_j and H'_k) protons, respectively. No formyl signal was observed. Signals, however, for the free dumbbell **1-H**·PF_6 were observed.

The fluorescence emission spectra (Fig. S15, ESI†) demonstrate that the anthracene fluorescence is quenched when the rotaxane is mixed with 10 equiv. of toluidine in MeCN. By contrast, the anthracene fluorescence can be observed when additional water or acid is added to the rotaxane in admixture with the toluidine. In a control experiment, we found that the anthracene fluorescence of **1-H**·PF_6 is not quenched on the addition of 1 equiv. of toluidine. Since the rotaxane–toluidine mixture contains the free dumbbell **1-H**·PF_6 (Fig. S9, ESI†) and, because of the fact that the anthracene fluorescence of **1-H**·PF_6 is quenched (Fig. S15, ESI†), it is reasonable to conclude that the newly formed (Scheme 5) diimine **5** with toluidine might have gained some additional supramolecular interactions with the dumbbell in close proximity[20]—as in the intermediates **IV** or **V**—leading to anthracene quenching. In addition, the effect of anthracene fluorescence was investigated by the addition of KPF_6, toluidine, water and acid in turn. The anthracene fluorescence (Fig. S16, ESI†) is observed only when acid is present in the system. These results confirm repeatedly that acid is crucial in order to be able to control the ON/OFF switching of the anthracene fluorescence in the mixed system containing the rotaxane.

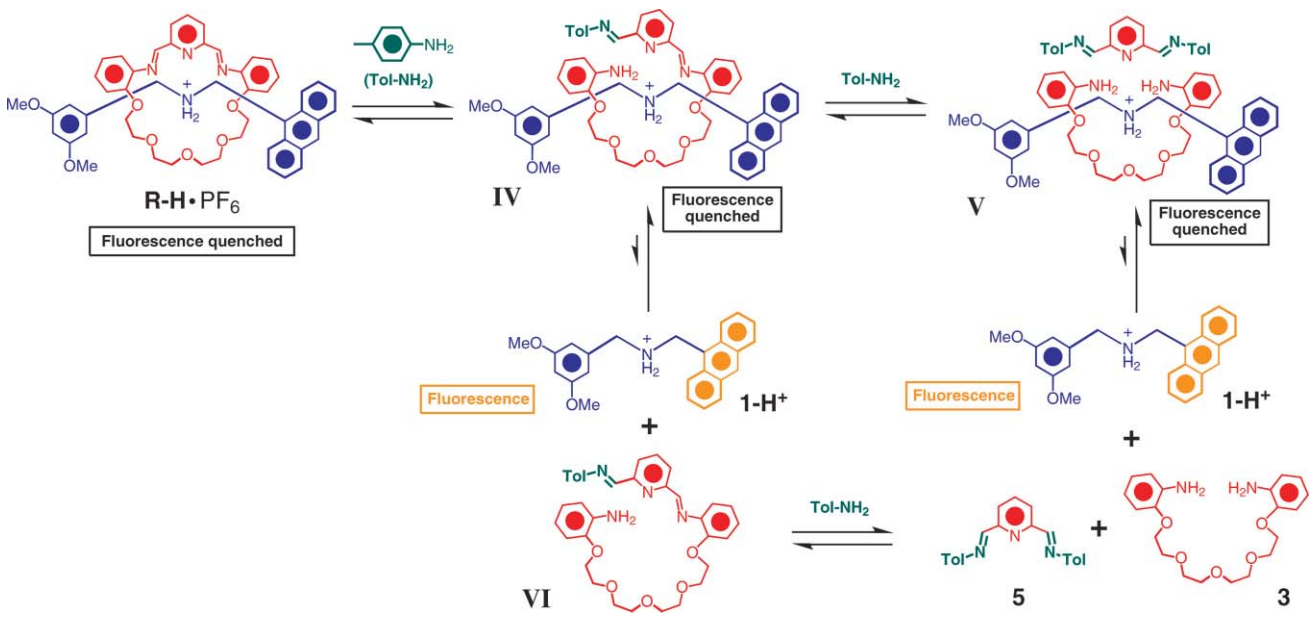

Scheme 5 Dissociation mechanism and fluorescence quenching properties of **R-H**·PF_6 in the presence of toluidine upon competitive exchange. The equilibrium favours formation of **R-H**·PF_6 or intermediates **IV** and **V**, wherein the anthracene fluorescence is quenched.

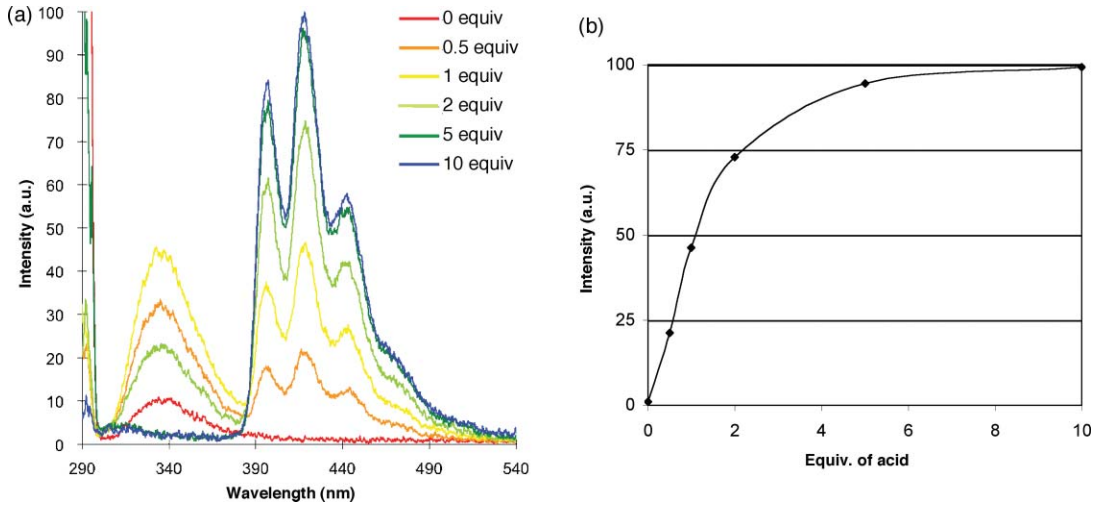

Fig. 9 (a) Stacked fluorescence emission of **R-H**·PF_6 with different amounts of HCl/H_2O (0.1 M). (b) A plot of fluorescence intensity at 418 nm *versus* equiv. of HCl/H_2O. Error = ±2%.

Molecular switching of the rotaxane at different acid concentrations

In a further set of experiments, the rotaxane was exposed to varying amounts of HCl/H_2O (1.0 M). To our surprise, the anthracene fluorescence intensities that are caused by treating the rotaxane with increasing amounts of HCl/H_2O result in a rise (Fig. 9a) in the fluorescence. This trend was witnessed very clearly in the range for 0–5 equiv. of HCl/H_2O (1.0 M). Only a relatively small difference in fluorescence intensity is evident, however, in the range of 5–10 equiv. of acid. Indeed, the increase (Fig. 9b) in the anthracene fluorescence intensity reaches a plateau, following a logarithmic curve. The anthracene fluorescence intensities in relation to the amount of HCl/Et_2O in the rotaxane were also investigated. The outcome (Fig. 10a) is very similar, except that the trend can be witnessed clearly from 0–10 equiv. of HCl/Et_2O (0.1 M). From the plot (Fig. 10b) of the anthracene fluorescence intensity *versus* the amount of HCl/Et_2O in the rotaxane solution, the anthracene fluorescence is directly proportional (linear) to the concentration of HCl/Et_2O. Clearly, the addition of acid to the rotaxane results in the dissociation of the anthracene-containing dumbbell, which on its own, gives an observable anthracene fluorescence signal. The rotaxane possesses not only an exclusive ON/OFF switch in the presence of acid, but also a switch with dimmer control, *i.e.*, the fluorescence intensity of anthracene—also the aminophenolic and 3,5-dimethoxybenzyl groups—can be fine-controlled by varying the concentration of the acid. An increase in acid concentration leads to an increase in anthracene fluorescence. Essentially, two acid sensors have been uncovered with different modes of dimmer control, *i.e.*, logarithmic (for HCl/H_2O) and linear (for HCl/Et_2O).

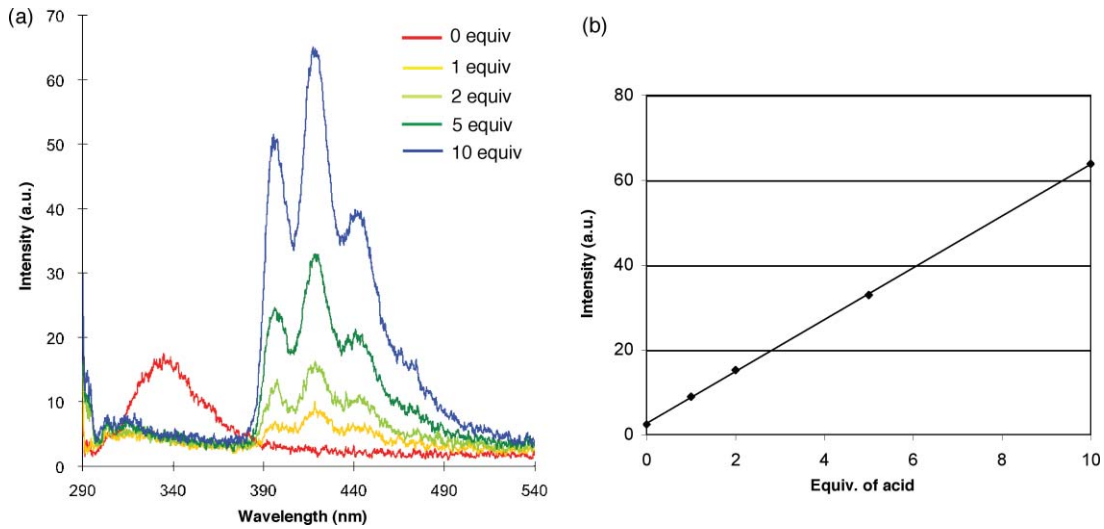

Fig. 10 (a) Stacked fluorescence emission of **R-H**·PF_6 with different amounts of HCl/Et_2O (0.1 M). (b) A plot of fluorescence intensity at 418 nm *versus* equiv. of HCl/Et_2O. Error = ±2%.

Table 1 Summary of the fluorescence output of the rotaxane **R-H**·PF_6 in the presence of four different additive inputs (H_2O, H^+, KPF_6, and Tol-NH_2). Input: "1" represents the presence of the additive while "0" represents the absence of the additive. Output: "1" represents observable fluorescence while "0" represents no observable fluorescence (fluorescence quenched). The output entries C, I, J, and O (parentheses) are somewhat uncertain since thoroughly dry conditions are unable to obtain

	Input				Output	
Entry	H_2O	H^+	KPF_6	Tol-NH_2	Anthracene fluorescence (418 nm, excitation = 290 nm)	Fluorescence at 330 nm (excitation = 290 nm)
A	0	0	0	0	0	1
B	1	0	0	0	0	1
C	0	1	0	0	(1)	(0)
D	0	0	1	0	0	1
E	0	0	0	1	0	1
F	1	1	0	0	1	0
G	1	0	1	0	0	1
H	1	0	0	1	0	1
I	0	1	1	0	(1)	(0)
J	0	1	0	1	(1)	(0)
K	0	0	1	1	0	1
L	1	1	1	0	1	0
M	1	1	0	1	1	0
N	1	0	1	1	0	1
O	0	1	1	1	(1)	(0)
P	1	1	1	1	1	0

Conclusion

A novel anthracene-containing dynamic [2]rotaxane-containing imine bonds has been synthesised in high yield by a three-component self-assembly process under templating—and characterised by ^{1}H NMR spectroscopy and mass spectrometry. The stability of the rotaxane has been investigated after the addition of water, acid, salt, and amine. The dissociation of the rotaxane has been monitored by observing the anthracene fluorescence and the chemical shifts in the ^{1}H NMR spectra. The dissociation rate for the rotaxane in the presence of acid is much faster than in the presence of water. Furthermore, the anthracene fluorescence of the rotaxane rises with increasing acid concentration. Two acid sensors have been identified with different modes of dimmer control—that is, logarithmic and linear. The use of a combination of stimuli for the rotaxane is summarized in Table 1, employing a binary notation with four different inputs and one output. Noticeably, the output entries E, F, G, and H are somewhat uncertain since we are unable to obtain thoroughly dry conditions. If the situation relating to the residual water molecules present in the solutions is overlooked, then the outputs can be interpolated (as the bracketed values). As a result, different molecular logic can be obtained by rational selections of certain specific input combinations.

Experimental

General methods

All chemicals were purchased from Aldrich or Acros and used without further purification. All solvents were dried, distilled and stored with molecular sieves (4 Å). Tetrahydrofuran (THF) was dried with Na–benzophenone. MeCN was dried with CaH_2; PhMe was dried with Na; and CH_2Cl_2 was dried with NaH. All reactions were performed under high purity nitrogen. Thin layer chromatography (TLC) was performed on silica gel 60 F254 (Merck). Column chromatography was performed on silica gel 60F (Merck 9385, 0.040–0.063 mm). Melting points were measured on an Electrothermal 9100 digital melting point apparatus and are uncorrected. UV/Visible absorption spectra were obtained using a Cary 5G UV-Vis-NIR spectrophotometer. Excitation and fluorescence spectra were recorded using a Hitachi F-4500 Fluorescence spectrophotometer. All nuclear magnetic resonance (NMR) spectra were recorded on Bruker Avance 400 (^{1}H: 400 MHz; ^{13}C: 101 MHz) spectrometer at 298 K and $CDCl_3$ was used as the solvent unless otherwise stated. The residual proton resonance signals of the non-deuterated solvents were used as reference calibration. Chemical shifts are reported as parts per million (ppm) for both ^{1}H and ^{13}C NMR spectroscopies. Electrospray ionization (ESI) mass spectra were measured on a Thermo Finnigan MAT95XL mass spectrometer with CH_2Cl_2–MeOH (1 : 1) as the mobile phase. The reported molecular mass (m/z) values correspond to the most abundant monoisotopic masses. For dissociation experiments, the initial rotaxane concentration was 0.02 M in MeCN.

Synthesis

The nitro compound **6**[21] was reduced (Scheme 6) to the aniline derivative **7** in the presence of hydrazine and palladium on charcoal in 93% yield. Then, two equivalents of **7** were treated with the dialdehyde **2** in the presence of molecular sieves (4 Å) to give the diimine **4** in 94% yield. Commercially available starting materials 9-anthraldehyde (**8**) and 3,5-dimethoxybenzylamine (**9**) were heated (Scheme 7) under reflux using a Dean–Stark apparatus for condensation, followed by reduction with $NaBH_4$. This reaction results in the formation of the amine thread **1** in 88% yield. Subsequently, **1** was protonated by careful addition of HPF_6 in H_2O, leading to the formation of the dumbbell **1-H$^+$** in 75% yield.

2-(2-(2-(2-Methoxyethoxy)ethoxy)ethoxy)aniline 7. 1-(2-(2-(2-Methoxyethoxy)ethoxy)ethoxy)-2-nitrobenzene (**6**) was prepared using the literature procedure.[21] A solution of the starting material (0.14 g, 0.50 mmol) in EtOH (10 mL) was added to wet Pd/C (catalytic amount) and hydrazine hydrate (0.10 mL, 3.21 mmol), and heated under reflux for 24 h. The resulting mixture was filtered

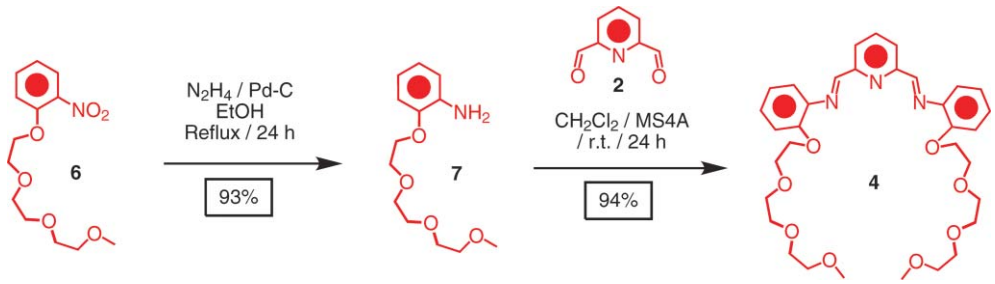

Scheme 6 Synthesis of compound **4**

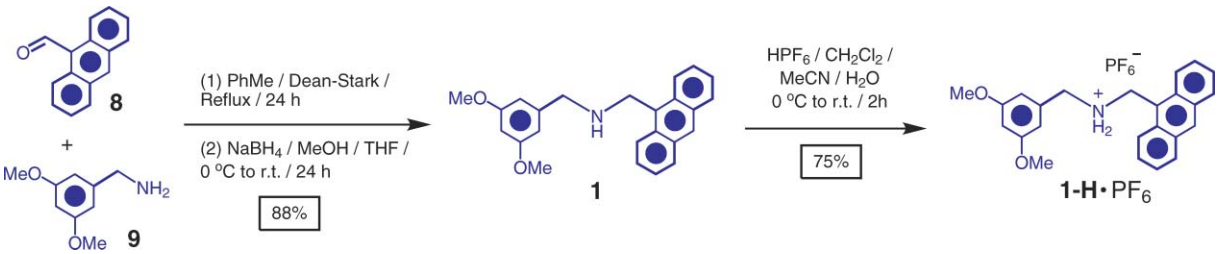

Scheme 7 Synthesis of the dumbbell **1-H**·PF_6

through a pad of Celite, washed with H_2O (5 mL) and extracted with CH_2Cl_2 (3 × 10 mL), dried ($MgSO_4$) and evaporated to dryness to give the product **7** as a faintly yellow liquid (0.12 g, 93%). ^{1}H NMR ($CDCl_3$, 400 MHz, 295 K) $\delta = 3.38$ (s, 3 H), 3.54–3.57 (m, 2 H), 3.65–3.69 (m, 4 H), 3.72–3.74 (m, 2 H), 3.84–3.86 (m, 2 H), 3.87–3.93 (br, 2 H), 4.14–4.17 (m, 2 H), 6.67–6.73 (m, 2 H), 6.78–6.82 (m, 2 H); ^{13}C NMR ($CDCl_3$, 101 MHz, 296 K): $\delta =$ 58.7, 68.1, 69.5, 70.3, 70.4, 70.5, 71.7, 112.8, 114.9, 117.8, 121.6, 137.1, 146.0; MS (HR-ESI): $C_{13}H_{21}NO_4$ $[M+Na]^+$: calcd 278.1363, found 278.1364.

Diimine 4. A solution of 2,6-pyridinedicarboxaldehyde (**2**) (0.03 g, 0.23 mmol) and 2-(2-(2-(2-methoxyethoxy)ethoxy)-ethoxy)aniline (**7**) (0.12 g, 0.46 mmol) in CH_2Cl_2 (5 mL) was stirred with molecular sieves (4 Å) for 24 h. Removal of molecular sieve and solvent gave the diimine **4** (0.14 g, 94%) as a yellow oil. ^{1}H NMR ($CDCl_3$, 400 MHz, 295 K): 3.33 (s, 6 H), 3.49 (t, $J = 4.6$ Hz, 4 H), 3.59–3.64 (m, 8 H), 3.75 (t, $J = 4.6$ Hz, 4 H), 3.89 (t, $J =$ 4.9 Hz, 4 H), 4.24 (t, $J = 4.9$ Hz, 4 H), 7.00–7.02 (m, 4 H), 7.13 (d, $J = 7.3$ Hz, 2 H), 7.20 (t, $J = 7.3$ Hz, 2 H), 7.92 (t, $J = 7.7$ Hz, 1 H), 8.31 (d, $J = 7.7$ Hz, 2 H), 8.70 (s, 2 H); ^{13}C NMR ($CDCl_3$, 101 MHz, 295 K): 59.0, 68.9, 69.7, 70.5, 70.7, 71.0, 71.9, 114.1, 121.0, 121.6, 122.9, 127.5, 137.1, 140.9, 151.6, 154.8, 161.2; MS (HR-ESI): $C_{33}H_{43}N_3O_8$ $[M+Na]^+$: calcd 632.2942, found 632.2940.

Amine 1. A solution of 9-anthraldehyde (**8**) (0.62 g, 2.99 mmol) and 3,5-dimethoxybenzylamine (**9**) (0.55 mL, 3.64 mmol) in PhMe (50 mL) was heated under reflux for 24 h using a Dean–Stark apparatus. The resulting solution was evaporated to dryness. The residue was dissolved in a mixture of MeOH–CH_2Cl_2 (2 : 1, 30 mL) and $NaBH_4$ (0.51 g, 13.40 mmol) added at 0 °C. After stirring the reaction mixture under ambient conditions for 24 h, the solvents were removed *in vacuo*, and the residue was partitioned between H_2O (50 mL) and CH_2Cl_2 (25 mL). The aqueous layer was further extracted with CH_2Cl_2 (3 × 25 mL). The combined organic extracts were dried ($MgSO_4$) and the resulting solution was evaporated to dryness. Flash column chromatography with hexane–EtOAc–Et_3N (150 : 50 : 1) on silica gel of the recovered product allowed isolation of the amine **1** (0.94 g, 88%) as a bright yellow powder. R_f 0.26 (hexane–EtOAc–Et_3N = 150 : 50 : 1); M.p. 85.4–87.1 °C; ^{1}H NMR ($CDCl_3$, 400 MHz, 296 K): $\delta = 3.82$ (s, 6 H), 3.99 (s, 2 H), 4.69 (s, 2 H), 6.42 (t, $J = 2.2$ Hz, 1 H), 6.62 (d, $J = 2.2$ Hz, 2 H), 7.44–7.52 (m, 4 H), 8.01 (d, $J = 7.7$ Hz, 2 H), 8.25 (d, $J =$ 8.8 Hz, 2 H), 8.41 (s, 1 H); ^{13}C NMR ($CDCl_3$, 101 MHz, 296 K): $\delta =$ 44.9, 54.5, 55.5, 99.5, 106.1, 124.3, 125.0, 126.1, 127.3, 129.2, 130.4, 131.7, 131.8, 143.1, 161.1; MS (HR-ESI): $C_{24}H_{23}NO_2$ $[M+H]^+$: calcd 358.1802, found 358.1799.

Dumbbell 1-H·PF_6. A solution of **1** (0.73 g, 2.05 mmol) in CH_2Cl_2–MeCN (3 : 1, 40 mL) was treated dropwise with 60 wt.% HPF_6 in H_2O (0.60 mL, 7.28 mmol) at 0 °C over a period of 5 min and stirred at ambient conditions for 2 h. The solvents were removed *in vacuo* to give a yellow solid, which was then dissolved in CH_2Cl_2 (40 mL), washed with H_2O (20 mL), further extracted with CH_2Cl_2 (3 × 10 mL) and dried (Na_2SO_4). The resulting solution was evaporated to give the product **1-H**·PF_6 as a milky yellow powder (0.78 g, 75%). M.p. >194 °C (decomposed); ^{1}H NMR (CD_3CN, 400 MHz, 296 K): $\delta = 3.80$ (s, 6 H), 4.41 (t, $J = 5.2$ Hz, 2 H), 5.24 (t, $J = 6.0$ Hz, 2 H), 6.61 (t, $J = 2.2$ Hz, 1 H), 6.69 (d, $J = 2.2$ Hz, 2 H), 7.12–7.50 (br, 2 H), 7.58–7.68 (m, 4 H), 8.10 (d, $J = 8.8$ Hz, 2 H), 8.16 (d, $J = 8.3$ Hz, 2 H), 8.74 (s, 1 H); ^{13}C NMR (CD_3CN, 101 MHz, 296 K, one aromatic signal is missing/overlapping): $\delta = 43.9$, 52.8, 56.3, 102.3, 109.1, 122.1, 124.1, 126.6, 128.6, 130.5, 131.8, 132.3, 133.4, 162.5; MS (HR-ESI): $C_{24}H_{24}F_6NO_2P$ $[M-PF_6]^+$: calcd 358.1802, found 358.1795.

Rotaxane R-H·PF_6. A solution of the dialdehyde **2** (0.04 g, 0.28 mmol), the diamine **3**[8c] (0.10 g, 0.28 mmol) and the dumbbell **1-H**·PF_6 (0.14 g, 0.28 mmol) in dry MeCN (0.46 mL, 60 mM) was stirred for 5 min at ambient temperature. Evaporation of

the solvent yielded the rotaxane **R-H**·PF_6 (94%) as a dull yellow solid. M.p. >163 °C (decomposed);^{1}H NMR (CD_3CN, 400 MHz, 295 K): 3.32 (s, 6 H), 3.59–3.84 (m, 10 H), 4.03–4.08 (m, 2 H), 4.29–4.31 (m, 4 H), 5.13 (t, J = 6.9 Hz, 2 H), 5.82 (t, J = 6.6 Hz, 2 H), 6.11 (t, J = 2.0 Hz, 1 H), 6.48 (d, J = 7.7 Hz, 2 H), 6.52 (d, J = 2.0 Hz, 2 H), 6.83 (t, J = 7.7 Hz, 2 H), 7.00–7.07 (m, 4 H), 7.15 (t, J = 7.4 Hz, 2 H), 7.24–7.28 (m, 4 H), 7.71 (t, J = 7.7 Hz, 1 H), 7.79 (d, J = 8.4 Hz, 2 H), 7.92 (s, 2 H), 8.35 (s, 1 H), 8.55 (d, J = 8.9 Hz, 2 H), 9.67–10.05 (br, 2 H); ^{13}C NMR (CD_3CN, 101 MHz, 295 K): 45.3, 53.3, 55.6, 69.2, 70.4, 71.8, 72.0, 100.9, 105.3, 112.9, 120.6, 122.2, 124.4, 124.9, 126.0, 127.3, 129.5, 129.6, 130.1, 130.5, 131.8, 132.1, 136.6, 139.5, 140.2, 152.8, 153.0, 160.1, 161.4; MS (HR-ESI): $C_{51}H_{53}F_6N_4O_7P$ [M–PF_6]$^+$: calcd 833.3909, found 833.3882.

Acknowledgements

This work was supported by a Strategic Investments Scheme from The Chinese University of Hong Kong and a General Research Fund (CUHK401808) by The Research Grants Council of Hong Kong.

References

1 (*a*) P. A. Brady, R. P. Bonar-Law, S. J. Rowan, C. J. Suckling and J. K. M. Sanders, *Chem. Commun.*, 1996, 319–320; (*b*) P. A. Brady and J. K. M. Sanders, *Chem. Soc. Rev.*, 1997, **26**, 327–336; (*c*) R. L. E. Furlan, S. Otto and J. K. M. Sanders, *Proc. Natl. Acad. Sci. USA*, 2002, **99**, 4801–4804; (*d*) J. K. M. Sanders, *Pure Appl. Chem.*, 2000, **72**, 2265–2274; (*e*) P. T. Corbett, J. Leclaire, L. Vial, K. R. West, J.-L. Wietor, J. K. M. Sanders and S. Otto, *Chem. Rev.*, 2006, **106**, 3652–3711; (*f*) J.-M. Lehn, *Chem. Eur. J.*, 1999, **5**, 2455–2463; (*g*) J.-M. Lehn, *Chem. Soc. Rev.*, 2007, **36**, 151–160; (*h*) S. J. Rowan, S. J. Cantrill, G. R. L. Cousins, J. K. M. Sanders and J. F. Stoddart, *Angew. Chem., Int. Ed.*, 2002, **41**, 898–952; (*i*) L. M. Greig and D. Philp, *Chem. Soc. Rev.*, 2001, **30**, 287–302; (*j*) A. Herrmann, *Org. Biomol. Chem.*, 2009, **7**, 3195–3204.

2 (*a*) K. S. Chichak, S. J. Cantrill, A. R. Pease, S. H. Chiu, G. W. V. Cave, J. L. Atwood and J. F. Stoddart, *Science*, 2004, **304**, 1308–1312; (*b*) S. J. Cantrill, K. S. Chichak, A. J. Peters and J. F. Stoddart, *Acc. Chem. Res.*, 2005, **38**, 1–9; (*c*) K. S. Chichak, S. J. Cantrill and J. F. Stoddart, *Chem. Commun.*, 2005, **27**, 3391–3393; (*d*) A. J. Peters, K. S. Chichak, S. J. Cantrill and J. F. Stoddart, *Chem. Commun.*, 2005, **27**, 3394–3396; (*e*) K. S. Chichak, A. J. Peters, S. J. Cantrill and J. F. Stoddart, *J. Org. Chem.*, 2005, **70**, 7956–7962; (*f*) C. D. Pentecost, A. J. Peters, K. S. Chichak, G. W. V. Cave, S. J. Cantrill and J. F. Stoddart, *Angew. Chem., Int. Ed.*, 2006, **45**, 4099–4104; (*g*) C. D. Pentecost, N. Tangchaivang, S. J. Cantrill, K. S. Chichak, A. J. Peters and J. F. Stoddart, *J. Chem. Ed.*, 2007, **84**, 855–859.

3 (*a*) K. C.-F. Leung, F. Aricó, S. J. Cantrill and J. F. Stoddart, *J. Am. Chem. Soc.*, 2005, **127**, 5808–5810; (*b*) K. C.-F. Leung, F. Aricó, S. J. Cantrill and J. F. Stoddart, *Macromolecules*, 2007, **40**, 3951–3959; (*c*) K. C.-F. Leung, *Macromol. Theory Simul.*, 2009, **18**, 328–335; (*d*) K. C.-F. Leung, S. Xuan and C.-M. Lo, *ACS Appl. Mater. Interfaces*, 2009, **1**, 2005–2012.

4 (*a*) A. R. Williams, B. H. Northrop, T. Chang, J. F. Stoddart, A. J. P. White and D. J. Williams, *Angew. Chem., Int. Ed.*, 2006, **45**, 6665–6669; (*b*) B. H. Northrop, N. Tangchiavang, J. D. Badjic and J. F. Stoddart, *Org. Lett.*, 2006, **8**, 3899–3902; (*c*) C. D. Pentecost, K. S. Chichak, A. J. Peters, G. W. V. Cave, S. J. Cantrill and J. F. Stoddart, *Angew. Chem., Int. Ed.*, 2007, **46**, 218–222; (*d*) J. Wu, K. C.-F. Leung and J. F. Stoddart, *Proc. Natl. Acad. Sci. USA*, 2007, **104**, 17266–17271; (*e*) L. M. Klivansky, G. Koshkakaryan, D. Cao and Y. Liu, *Angew. Chem., Int. Ed.*, 2009, **48**, 4185–4189.

5 (*a*) D. Philp and J. F. Stoddart, *Angew. Chem., Int. Ed.*, 1996, **35**, 1155–1196; (*b*) F. Aricó, J. D. Badjic, S. J. Cantrill, A. H. Flood, K. C.-F. Leung, Y. Liu and J. F. Stoddart, *Top. Curr. Chem.*, 2005, **249**, 203–259; (*c*) K. E. Griffiths and J. F. Stoddart, *Pure Appl. Chem.*, 2008, **80**, 485–506; (*d*) J. F. Stoddart and H. M. Colquhoun, *Tetrahedron*, 2008, **64**, 8231–8263.

6 For examples of rotaxane syntheses with ring closing metathesis, see: (*a*) J. A. Wisner, P. D. Beer, M. G. B. Drew and M. R. Sambrook, *J. Am. Chem. Soc.*, 2002, **124**, 12469–12476; (*b*) A. F. M. Kilbinger, S. J. Cantrill, A. W. Waltman, M. W. Day and R. H. Grubbs, *Angew. Chem., Int. Ed.*, 2003, **42**, 3281–3285; (*c*) F. Aricó, P. Mobian, J.-M. Kern and J.-P. Sauvage, *Org. Lett.*, 2003, **11**, 1887–1890; (*d*) J. D. Badjic, S. J. Cantrill, R. H. Grubbs, E. N. Guidry, R. Orenes and J. F. Stoddart, *Angew. Chem., Int. Ed.*, 2004, **43**, 3273–3278; (*e*) E. N. Guidry, S. J. Cantrill, J. F. Stoddart and R. H. Grubbs, *Org. Lett.*, 2005, **7**, 2129–2132; (*f*) S. J. Cantrill, R. H. Grubbs, D. Lanari, K. C.-F. Leung, A. Nelson, K. G. Poulin-Kerstien, S. P. Smidt, J. F. Stoddart and D. A. Tirrell, *Org. Lett.*, 2005, **7**, 4213–4216; (*g*) H. Hou, K. C.-F. Leung, D. Lanari, A. Nelson, J. F. Stoddart and R. H. Grubbs, *J. Am. Chem. Soc.*, 2006, **128**, 15358–15359; (*h*) E. N. Guidry, J. Li, S. J. Cantrill, J. F. Stoddart and R. H. Grubbs, *J. Am. Chem. Soc.*, 2007, **129**, 8944–8945.

7 For rotaxane-containing disulfide units in their dumbbell-shaped components that are formed by riveting and stoppering approaches, see: (*a*) A. G. Kolchinski, N. W. Alcock, R. A. Roesner and D. H. Busch, *Chem. Commun.*, 1998, 1437–1438; (*b*) Y. Furusho, T. Hasegawa, A. Tsuboi, N. Kihara and T. Takata, *Chem. Lett.*, 2000, 18–19; (*c*) T. Oku, T. Furush and T. Takata, *J. Polym. Sci. Part A*, 2003, **41**, 119–123; (*d*) Y. Furusho, T. Oku, G. A. Rajkumar and T. Takata, *Chem. Lett.*, 2004, **33**, 52–53.

8 (*a*) S. J. Cantrill, S. J. Rowan and J. F. Stoddart, *Org. Lett.*, 1999, **1**, 1363–1366; (*b*) S. J. Rowan and J. F. Stoddart, *Org. Lett.*, 1999, **1**, 1913–1916; (*c*) P. T. Glink, A. I. Oliva, J. F. Stoddart, A. J. P. White and D. J. Williams, *Angew. Chem., Int. Ed.*, 2001, **40**, 1870–1875; (*d*) M. Horn, J. Ihringer, P. T. Glink and J. F. Stoddart, *Chem. Eur. J.*, 2003, **17**, 4046–4054; (*e*) F. Aricó, T. Chang, S. J. Cantrill, S. I. Khan and J. F. Stoddart, *Chem. Eur. J.*, 2005, **11**, 4655–4666; (*f*) C. D. Meyer, C. S. Joiner and J. F. Stoddart, *Chem. Soc. Rev.*, 2007, **36**, 1705–1723; (*g*) P. C. Haussmann, S. I. Khan and J. F. Stoddart, *J. Org. Chem.*, 2007, **72**, 6708–6713; (*h*) P. C. Haussmann and J. F. Stoddart, *Chem. Rec.*, 2009, **9**, 136–154; (*i*) K. C.-F. Leung, W.-Y. Wong, F. Aricó, P. C. Haussmann and J. F. Stoddart, *Org. Biomol. Chem.*, 2010, **8**, 83–89.

9 (*a*) C. Godoy-Alcántar, A. K. Yatsimirsky and J.-M. Lehn, *J. Phys. Org. Chem.*, 2005, **18**, 979–985; (*b*) W. Lu and T. H. Chang, *J. Org. Chem.*, 2001, **66**, 3467–3473; (*c*) T. Hirashita, Y. Hayashi, K. Mitsui and S. Araki, *J. Org. Chem.*, 2003, **68**, 1309–1313.

10 (*a*) V. Saggiomo and U. Lüning, *Eur. J. Org. Chem.*, 2008, 4329–4333; (*b*) V. Saggiomo and U. Lüning, *Tetrahedron Lett.*, 2009, **50**, 4663–4665.

11 A. Simion, C. Simion, T. Kanda, S. Nagashima, Y. Mitoma, T. Yamada, K. Mimura and M. Tashiro, *J. Chem. Soc. Perkin Trans. 1*, 2001, 2071–2078.

12 M. Hutin, C. A. Schalley, G. Bernardinelli and J. R. Nitschke, *Chem. Eur. J.*, 2006, **12**, 4069–4076.

13 K. C.-F. Leung, C.-P. Chak, C.-M. Lo, W.-Y. Wong, S. Xuan and C. H. K. Cheng, *Chem. Asian J.*, 2009, **4**, 364–381.

14 (*a*) S. R. Quake and A. Scherer, *Science*, 2000, **290**, 1536–1540; (*b*) J. Atencia and D. J. Beebe, *Nature*, 2005, **437**, 648–655; (*c*) P. S. Dittrich, K. Tachikawa and A. Manz, *Anal. Chem.*, 2006, **78**, 3887–3907.

15 (*a*) V. Balzani, M. Clemente-León, A. Credi, B. Ferrer, M. Venturi, A. H. Flood and J. F. Stoddart, *Proc. Natl. Acad. Sci. USA*, 2006, **103**, 1178–1183; (*b*) B. Ferrer, G. Rogez, A. Credi, R. Ballardini, M. T. Gandolfi, V. Balzani, Y. Liu, H.-R. Tseng and J. F. Stoddart, *Proc. Natl. Acad. Sci. USA*, 2006, **103**, 18411–18416; (*c*) S. Saha, K. C.-F. Leung, T. D. Nguyen, J. F. Stoddart and J. I. Zink, *Adv. Funct. Mater.*, 2007, **17**, 685–693; (*d*) T. D. Nguyen, K. C.-F. Leung, M. Liong, Y. Liu, J. F. Stoddart and J. I. Zink, *Adv. Funct. Mater.*, 2007, **17**, 2101–2110.

16 (*a*) L. Kovbasyuk and R. Kramer, *Chem. Rev.*, 2004, **104**, 3161–3187; (*b*) J. F. Callan, A. P. de Silva and D. C. Magri, *Tetrahedron*, 2005, **61**, 8551–8588; (*c*) W. R. Browne and B. L. Feringa, *Nat. Nanotechnol.*, 2006, **1**, 25–35; (*d*) A. B. Descalzo, R. Martínez-Máñez, F. Sancenón, K. Hoffmann and K. Rurack, *Angew. Chem., Int. Ed.*, 2006, **45**, 5924–5948; (*e*) E. R. Kay, D. A. Leigh and F. Zerbetto, *Angew. Chem., Int. Ed.*, 2007, **46**, 72–191; (*f*) T. Cheng, D. I. Rozkiewicz, B. J. Ravoo, E. W. Meijer and D. N. Reinhoudt, *Nano Lett.*, 2007, **7**, 978–980; (*g*) J. F. Stoddart, *Chem. Soc. Rev.*, 2009, **38**, 1802–1820.

17 (*a*) P. R. Ashton, R. Ballardini, V. Balzani, M. Gómez-López, S. E. Lawrence, M. V. Martínez-Díaz, M. Montalti, A. Piersanti, L. Prodi, J. F. Stoddart and D. J. Williams, *J. Am. Chem. Soc.*, 1997, **119**,

10641–10651; (*b*) P. R. Ashton, R. Ballardini, V. Balzani, I. Baxter, A. Credi, M. C. T. Fyfe, M. T. Gandolfi, M. Gómez-López, M. V. Martínez-Díaz, A. Piersanti, N. Spencer, J. F. Stoddart, M. Venturi, A. J. P. White and D. J. Williams, *J. Am. Chem. Soc.*, 1998, **120**, 11932–11942; (*c*) R. Ballardini, V. Balzani, W. Dehaen, A. E. Dell'Erba, F. M. Raymo, J. F. Stoddart and M. Venturi, *Eur. J. Org. Chem.*, 2000, 591–602; (*d*) S. Garaudée, S. Silvi, M. Venturi, A. Credi, A. H. Flood and J. F. Stoddart, *ChemPhysChem*, 2005, **6**, 2145–2152; (*e*) S. Saha, L. E. Johansson, A. H. Flood, H.-R. Tseng, J. I. Zink and J. F. Stoddart, *Small*, 2005, **1**, 87–90; (*f*) S. Saha, L. E. Johansson, A. H. Flood, H.-R. Tseng, J. I. Zink and J. F. Stoddart, *Chem. Eur. J.*, 2005, **11**, 6846–6858; (*g*) S. Saha and J. F. Stoddart, *Chem. Soc. Rev.*, 2007, **36**, 77–92.

18 R. A. Bissell, A. P. de Silva, H. Q. N. Gunaratne, P. L. M. Lynch, G. E. M. Maguire, C. P. McCoy and K. R. A. S. Sandanayake, *Top. Curr. Chem.*, 1993, **168**, 223–264.

19 (*a*) K. C.-F. Leung, T. D. Nguyen, J. F. Stoddart and J. I. Zink, *Chem. Mater.*, 2006, **18**, 5919–5928; (*b*) R. Liu, Y. Zhang and P. Feng, *J. Am. Chem. Soc.*, 2009, **131**, 15128–15129.

20 (*a*) By NMR titration between the dumbbell **1-H**$^+$ and diimine compound **5**, a Job plot has been created (unpublished results). The plot reveals that the dumbbell **1-H**$^+$ and diimine compound **5** formed a 1 : 1 supramolecular complex.

21 M. Kimura, K. Kajita, N. Onoda and S. Morosawa, *J. Org. Chem.*, 1990, **55**, 4887–4892.